Int. J. Anal. Appl. (2025), 23:81

International Journal of Analysis and Applications

Modelling and Optimal Control of Influenza Dynamics with Structured Populations Based on Education and Isolation

Samson Olaniyi[1], Idris A. Lawal[1], Ramoshweu S. Lebelo[2], Furaha M. Chuma[3], Sulaimon F. Abimbade[1]

[1]*Department of Pure and Applied Mathematics, Ladoke Akintola University of Technology, Ogbomoso, Nigeria*

[2]*Department of Applied Physical Sciences, Vaal University of Technology, Vanderbijilpark, South Africa*

[3]*Department of Physics, Mathematics and Informatics, Dar es Salaam University College of Education, Tanzania*

[*]*Corresponding author:* sfabimbade81@lautech.edu.ng

Abstract. This paper presents a new mathematical model for the transmission of avian influenza virus dynamics with education-structured susceptible and isolation-structured infectious human populations in the presence of vaccination. Several dynamical systems methodologies are employed to analyse the avian influenza in human-bird interacting populations. The fundamental properties exhibited by the model are assessed through the theory of positivity and boundedness of solutions. The effective reproduction number, $\mathcal{R}_e$, that measures the spread potential of the influenza infection is calculated using the next generation matrix approach. Metzler matrix approach and Lyapunov function are employed to investigate the global asymptotic dynamics of the model about its influenza-free and endemic states, respectively. Furthermore, the model is extended to accommodate four time-dependent control interventions, such as public awareness campaign, vaccination, treatment with anti-viral drugs, and birds culling strategy. By applying Pontryagin's maximum principle, the optimal control quadruple are characterized. Specifically, combinations of any three of the control interventions are explored in forestalling the transmission of avian influenza in the population. The findings of the study do not only reveal various parameters of the model to be targeted for prevention and control of the disease, but also show the importance of consolidating control efforts in the fight against the avian influenza disease.

1. Introduction

Influenza viruses are a group of ribonucleic acid (RNA) viruses responsible for certain respiratory infections in humans, avians, and other animals. The origin of these viruses is rooted in

Received: Jan. 28, 2025.

2020 *Mathematics Subject Classification.* 92B05, 34D20, 34H05.

Key words and phrases. Avian Influenza; Structured mathematical model; Effective reproduction number; Global stability; Optimal control.

https://doi.org/10.28924/2291-8639-23-2025-81
ISSN: 2291-8639

their evolution and adaptation across different species. Influenza viruses are part of the *Orthomyxoviridae* family, characterized by segmented RNA genomes. There are four types of influenza viruses namely, Influenza A which is known for its ability to infect a wide range of hosts and it is sub-classified into hemagglutinin (H) and neuraminidase (N) subtypes based on two surface proteins [1]. The variability in these proteins is the source of the different subtypes, such as H1N1, H3N2, and H5N1; Influenza B, which primarily infects humans and does not have subtypes, but tends to cause localized epidemics rather than pandemics; Influenza C has a more stable genome and typically causes mild respiratory illness, primarily in children; and Influenza D which is less common and mainly affects cattle. Influenza viruses have a zoonotic origin, implying transmission between animals and humans [2]. Influenza A viruses, in particular, have a wide host range, including avians, pigs, horses, seals, and humans. Wild avians, especially aquatic avians like ducks, are considered the primary natural reservoir for influenza A. These avians harbor a wide variety of asymptomatic influenza strains [1,3].

Influenza viruses have a segmented RNA genome with eight separate pieces of genetic material. This structure allows for genetic re-assortment when two different influenza viruses infect the same host cell. This can result in a new virus strain with a mix of genetic material from each parent virus, potentially leading to significant changes in virulence and transmissibility. Influenza viruses spread through respiratory droplets when an infected person coughs, sneezes, or talks [3,4]. The virus can also survive on surfaces for a limited time, leading to fomite transmission. This high transmissibility combined with the virus's ability to mutate and adapt, contribute to the widespread and recurring nature of influenza outbreaks [5]. Antigenic shift and drift are two key processes serving as a steering wheel for the evolution and diversity of influenza viruses in the population. On the one hand, antigenic drift involves gradual mutations in the viral genome, particularly in the genes encoding the surface proteins hemagglutinin (HA) and neuraminidase (NA). These mutations allow the virus to evade the host's immune system over time, leading to seasonal influenza outbreaks. While antigenic shift on the other hand occurs when two different influenza A viruses infect the same host cell and exchange genetic segments, resulting in a new viral subtype. This process can lead to significant changes in the virus's surface proteins, sometimes resulting in pandemics when the new subtype is highly transmissible and the population lacks immunity against it [6,7].

In summary, the origin of influenza viruses lies in their ability to mutate and re-assort among different species. These processes enable the viruses to evolve and adapt, leading to seasonal outbreaks and occasionally, pandemics when significant changes occur. Therefore, understanding this origin helps in designing effective interventions for monitoring, preventing and vaccinating against the viral infection. To this end, quite a number of medical efforts have been put in place to understand the intricacies associated with the evolution of avian influenza in human population. In addition to these medical efforts, several authors in the literature have used mathematical modelling tools to study influenza virus dynamics, see for instance, [8–22] and some

of the references therein. In [9], the influence of psychological effect on the spread dynamics of avian influenza virus was investigated using a deterministic mathematical model with saturated incidence. A mathematical model featuring psychological effect, saturation inhibition effect and nonlinear treatment was proposed to study the transmission dynamics of avian influenza in [11]. The impact of matching and mismatching between vaccine strains and circulating strains of influenza in annual hajj exercise was studied in [12]. Baba and associates [13] stressed on the impact of resistant and non-resistant strains on the transmission dynamics of influenza.

In another development, Barik and his colleagues in [14] designed an optimal control framework for the dynamics of avian influenza in different geographical areas. Du *et al.* [15] applied mathematical modelling to the co-dynamics of influenza and COVID-19 in human population using a system of ordinary differential equations. The authors in [17] applied mathematical modelling to the study of a within-host influenza dynamics. In attempt to understand the mechanisms behind the dynamics of avian influenza with special interest in proffering effective control strategies that could be adopted in setting the viral infection to extinction in the population, authors in [18] designed an optimal control framework featuring three time-dependent control intervention strategies representing public awareness programs, treatment, and psychological support to stem the transmission dynamics of avian influenza virus in the population. Recently, authors in [19] conducted a robust comparative study on the evolution of avian influenza in chicken farms with vaccination and seasonality effects. While the study of avian influenza virus in a live avian market was conducted in [20] by fitting the model to real data of avian influenza virus from a field experiment in Bangladesh. In a similar and more recent development, Andreu-Vilarroig and colleagues [21] studied the transmission dynamics of avian influenza with variation in vaccinated and non-vaccinated populations purposely to gain further insights into the spread dynamics of the infection.

It should be mentioned that in developing countries, the level of acquaintance of individuals with opportunistic infections such as the viral infection under study is very important in designing control measures that would assist in completely eradicating the infection in the population. Most studies on the dynamics of avian influenza virus in the literature did not consider classification of their mathematical models into different categories based on their level of acquaintance with the virus. This study, therefore, proposes a new mathematical model focusing on the stratification of the total human population into different classifications to gain further insights into the transmission dynamics of avian influenza in human population. The susceptible human population is sub-classified into informed and uninformed susceptible individuals and the infectious population is stratified into isolated and non-isolated infectious individuals. The organization of the other aspects of the study are structured as follows: Section 2 presents the mathematical formulation of the avian influenza model. Robust qualitative analysis of the autonomous nonlinear avian influenza model is conducted in Section 3. Section 4 is concerned with the analysis of the

non-autonomous version of the nonlinear avian influenza model with discussion. And Section 5 concludes the study.

2. Avian Influenza Model

It is important to bear in mind that the transmission dynamics of avian influenza virus stems from the interaction between human and avians populations. To this end, the total human population, $N_h(t)$, is compartmentalized into six mutually exclusive populations, namely uninformed susceptible represented by $S_u(t)$ (those who are not educated or informed about the disease and are prone to contracting the viral infection), informed susceptible population denoted by $S_i(t)$ (individuals who are educated and fully informed about the disease but still have the likelihood of contracting the viral infection), population of vaccinated informed individuals represented by $V(t)$ (population of informed susceptible individuals who are vaccinated against the viral infection), non-isolated infectious population designated by $I_{1h}(t)$ (population of actively infected individuals who are not in isolation), population of infectious individuals in isolation duly represented by $I_{2h}(t)$ (population of symptomatically infectious individuals who are in isolation, but have the likelihood of not spreading the infection instantaneously due to restriction in their interaction), and recovered class delineated by $R(t)$ (population of infectious individuals who recovered after receiving anti-influenza viral treatment). Thus, the total human population is given by

$$N_h(t) = S_u(t) + S_i(t) + V(t) + I_{1h}(t) + I_{2h}(t) + R(t). \tag{2.1}$$

The uninformed susceptible population is assumed to increase at a recruitment rate, represented by Λ_h, and the population is reduced by a force of infection $\beta_h(I_{1h} + I_b + \theta I_{2h})$, where β_h is the effective contact rate, and $\theta \in (0, 1)$ is the modification parameter measuring the degree of infectivity in isolated infectious human over non-isolated actively infected humans. Therefore, it makes sense to assume that the infectious individuals in isolation transmit infection at a more reduced rate compared to non-isolated infectious individuals. Moreover, the uninformed susceptible population becomes fully acquainted (informed) individuals at a rate α. The population is further diminished by natural mortality at a rate μ. Therefore, the dynamics of the uninformed susceptible population with time is given by

$$\frac{dS_u}{dt} = \Lambda_h - \beta_h \left(I_{1h} + I_b + \theta I_{2h}\right) S_u - (\alpha + \mu_h) S_u. \tag{2.2}$$

The population of educated or informed susceptible individuals is built up by the progression of uninformed susceptible individuals due to proper education at a rate α. The population is reduced by the force of infection at a modified rate $(1-\psi)\beta_h(I_{1h} + I_b + \theta I_{2h})$, where $(1-\psi) > 0$ measures the level of adherence to educational informations acquired during sensitization on the disease. In attempt to curb the spread of the viral infection, the population is further downsized at per capita vaccination rate σ and natural death rate μ. Therefore, the rate of change of the informed

susceptible individuals is given by

$$\frac{dS_i}{dt} = \alpha Su - (1-\psi)\beta_h \left(I_{1h} + I_b + \theta I_{2h}\right) S_i - (\sigma + \mu_h)S_i. \tag{2.3}$$

Following effective sensitization of the susceptible class, a fraction, denoted by σ, of the informed susceptible individuals gets vaccinated and directly join the vaccinated class. The vaccinated population is diminished at the per capita natural mortality rate μ. Thus, the rate of change of the population is given by

$$\frac{dV}{dt} = \sigma S_i - \mu_h V. \tag{2.4}$$

The population of the non-isolated infectious individual is generated by the forces of infection $\beta_h(I_{1h} + I_b + \theta I_{2h})$ and $(1-\psi)\beta_h(I_{1h} + I_b + \theta I_{2h})$. The population diminishes by isolation of infectious human at a rate ρ and further reduces by the spontaneous recovery of infectious human at a rate τ_1. The population is also reduced by natural mortality at rate μ. Therefore, the rate of change of the non-isolated infectious human is given by

$$\frac{dI_{1h}}{dt} = \beta_h \left(I_{1h} + I_b + \theta I_{2h}\right) S_u + (1-\psi)\beta_h \left(I_{1h} + I_b + \theta I_{2h}\right) S_i - (\rho + \tau_1 + \mu_h)I_{1h}. \tag{2.5}$$

As a consequence of isolation of infectious human at a rate ρ, the population of infectious human in isolation is developed. The population reduces due to recovery at a rate τ_2, and further reduced at the per capita natural mortality rate μ. Therefore, the evolution of infectious human in isolation is given by

$$\frac{dI_{2h}}{dt} = \rho I_{1h} - (\tau_2 + \mu_h)I_{2h}. \tag{2.6}$$

The population of recovered human is generated by the recovery of non-isolated and isolated infectious humans, respectively, at rates τ_1 and τ_2. The population is reduced by the per capita natural mortality rate μ. Hence, the rate of change of the recovered population is given by

$$\frac{dR}{dt} = \tau_1 I_{1h} + \tau_2 I_{2h} - \mu_h R. \tag{2.7}$$

Since the transmission dynamics of avian influenza virus involves the interaction between human and avian or bird populations, the total bird population represented by $N_b(t)$ is stratified into the populations of susceptible $S_b(t)$ and infectious birds $I_b(t)$. So that the total bird population is expressed as

$$N_b(t) = S_b(t) + I_b(t). \tag{2.8}$$

The susceptible bird population is assumed to increase at a recruitment rate, represented by Λ_b. Following effective contact with infectious bird, the population is reduced by a mass action incidence function $\beta_b S_b I_b$, where β_b is the transmission probability of infection from an infectious bird to a susceptible bird. The population is further downsized by the natural mortality rate μ_b. Therefore, the rate of change of susceptible bird population is given by

$$\frac{dS_b}{dt} = \Lambda_b - \beta_b S_b I_b - \mu_b S_b. \tag{2.9}$$

Following effective contact with infectious bird, the population of infectious bird is built by a mass action incidence function $\beta_b S_b I_b$, and the population is downsized by the natural mortality rate μ_b. Thus, the evolution of infectious birds population is given by

$$\frac{dI_b}{dt} = \beta_b S_b I_b - \mu_b I_b. \tag{2.10}$$

The schematic diagram depicting the flow between the human and bird compartments is given in Figure 1. As a consequence of the foregoing assumptions and coupling all the equations together, the eight-dimensional system of nonlinear ordinary differential equations describing the time evolution of avian influenza virus in human-bird interacting populations is obtained as follows.

$$\begin{aligned}
\frac{dS_u}{dt} &= \Lambda_h - \beta_h \left(I_{1h} + I_b + \theta I_{2h}\right) S_u - (\alpha + \mu_h) S_u, \\
\frac{dS_i}{dt} &= \alpha Su - (1-\psi)\beta_h \left(I_{1h} + I_b + \theta I_{2h}\right) S_i - (\sigma + \mu_h) S_i, \\
\frac{dV}{dt} &= \sigma S_i - \mu_h V, \\
\frac{dI_{1h}}{dt} &= \beta_h \left(I_{1h} + I_b + \theta I_{2h}\right) \left(S_u + (1-\psi) S_i\right) - (\rho + \tau_1 + \mu_h) I_{1h}, \\
\frac{dI_{2h}}{dt} &= \rho I_{1h} - (\tau_2 + \mu_h) I_{2h}, \\
\frac{dR}{dt} &= \tau_1 I_{1h} + \tau_2 I_{2h} - \mu_h R, \\
\frac{dS_b}{dt} &= \Lambda_b - \beta_b S_b I_b - \mu_b S_b, \\
\frac{dI_b}{dt} &= \beta_b S_b I_b - \mu_b I_b,
\end{aligned} \tag{2.11}$$

with non-negative initial conditions,

$$\begin{aligned}
&S_u(0) = S_{u_0},\ S_i(0) = S_{i_0},\ V(0) = V_0,\ I_{1h}(0) = I_{1h_0}, \\
&I_{2h}(0) = I_{2h_0},\ R(0) = R_0,\ S_b(0) = S_{b_0},\ I_b(0) = I_{b_0}.
\end{aligned} \tag{2.12}$$

Complete descriptions of the variables and parameters associated with the system (2.11) are provided in Table 1 and Table 2, respectively.

3. Analysis of the Influenza Model

This section is dedicated to the qualitative analysis of the nonlinear mathematical model describing the transmission dynamics of avian influenza virus in the population.

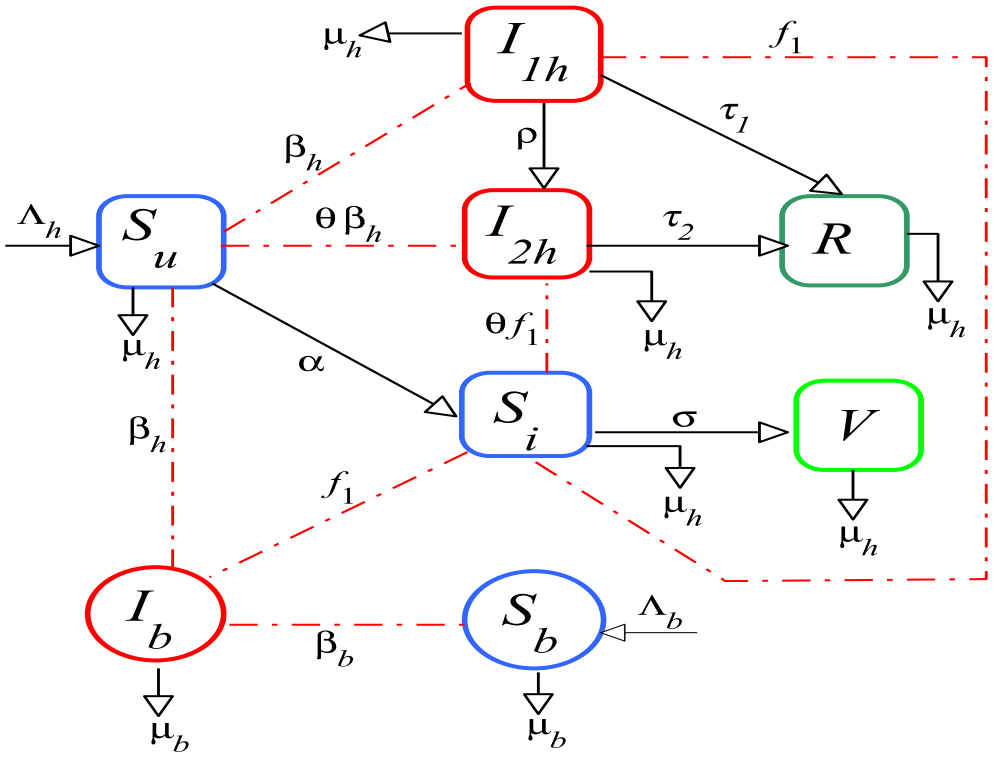

FIGURE 1. The schematic flow of avian influenza virus transmission in human-bird interacting populations, where $f_1 = (1-\psi)\beta_h$.

TABLE 1. Description of variables of the avian influenza model.

	Description
$S_u(t)$	Population of uniformed susceptible humans
$S_i(t)$	Population of informed susceptible humans
$V(t)$	Population of vaccinated humans
$I_{1h}(t)$	Population of non-isolated infectious humans
$I_{2h}(t)$	Population of isolated infectious humans
$R(t)$	Population of recovered humans
$N_h(t)$	Total human population
$S_b(t)$	Population of susceptible birds
$I_b(t)$	Population of infectious birds
$N_b(t)$	Total bird population

3.1. **Positivity of solutions.** Since the nonlinear mathematical model (2.11) involves the dynamics of avian influenza virus in human-bird interacting populations, it is imperative to establish that all the state variables of the model are non-negative. Noting that the model parameters are non-negative.

TABLE 2. Description of parameters of the avian influenza model.

	Description
Λ_h	Recruitment rate of human population
Λ_b	Recruitment rate of bird population
β_h	Transmission probability of infection in humans
β_b	Transmission probability of infection in birds
μ_h	Natural mortality rate of humans
μ_b	Natural mortality rate of birds
α	Progression rate of uninformed susceptible to informed class
τ_1	Spontaneous recovery rate in I_{1h}
θ	Modification parameter due to infectiousness in I_{2h}
ψ	Rate of adherence to precautionary education
τ_2	Recovery rate due to treatment
σ	Vaccination rate of informed susceptible individuals
ρ	Progression rate of non-isolated infectious human to isolation

Theorem 3.1. *Given that* $S_{u_0} \geq 0$, $S_{i_0} \geq 0$, $V_0 \geq 0$, $I_{1h_0} \geq 0$, $I_{2h_0} \geq 0$, $R_0 \geq 0$, $S_{b_0} \geq 0$, $I_{b_0} \geq 0$, *then the solution set,* $\{S_u, S_i, V, I_{1h}, I_{2h}, S_b, I_b\}$, *of the avian influenza model* (2.11) *remains non-negative for all times,* $t > 0$.

Proof. The first compartment of the avian influenza model (2.11) yields the following differential inequality

$$\frac{dS_u}{dt} \geq -(\beta_h (I_{1h} + I_b + \theta I_{2h}) + (\alpha + \mu_h))S_u. \tag{3.1}$$

So that

$$\frac{d}{dt}\left[S_u \exp\left(\int_0^t \beta_h (I_{1h}(\varphi) + I_b(\varphi) + \theta I_{2h}(\varphi))\, d\varphi + (\alpha + \mu_h)t\right)\right] > 0. \tag{3.2}$$

It therefore follows that,

$$S_u \geq S_{u_0} \exp\left[-\left(\int_0^t \beta_h (I_{1h}(\varphi) + I_b(\varphi) + \theta I_{2h}(\varphi))\, d\varphi + (\alpha + \mu_h)t\right)\right] > 0, \forall t > 0. \tag{3.3}$$

It can be shown through similar procedure that the remaining state variables of the avian influenza model (2.11) are non-negative for all times. Hence, the solution set is non-negative $\forall\ t > 0$. □

3.2. **Equilibria and effective reproduction number.**

3.2.1. *Disease-free and effective reproduction number.* In the absence of infection cases in human and bird populations, the influenza-free (disease-free) steady state of the avian influenza model (2.11), represented by $\mathcal{E}_0$, is given by

$$\mathcal{E}_0 = (S_u^0, S_i^0, V^0, 0, 0, 0, S_b^0, 0), \tag{3.4}$$

where

$$S_u^0 = \frac{\Lambda_h}{\alpha + \mu_h},\ S_i^0 = \frac{\alpha\Lambda_h}{(\sigma + \mu_h)(\alpha + \mu_h)},\ V^0 = \frac{\sigma\alpha\Lambda_h}{\mu_h(\sigma + \mu_h)(\alpha + \mu_h)},\ S_b^0 = \frac{\Lambda_b}{\mu_b}.$$

In what follows, the effective reproduction number, $\mathcal{R}_e$, of the influenza model (2.11), which is an important metric for measuring the spread strength of diseases epidemiologically, is calculated using the well-known next generation operator [24, 25]. Two important matrices F (of the new infection terms) and V (of the transition terms) evaluated at the influenza-free equilibrium point (3.4), respectively, are given by

$$F = \begin{pmatrix} \frac{\beta_h(\Lambda_h k_2 + (1-\psi)\alpha\Lambda_h)}{k_1 k_2} & \frac{\theta\beta_h(\Lambda_h k_2 + (1-\psi)\alpha\Lambda_h)}{k_1 k_2} & \frac{\beta_h(\Lambda_h k_2 + (1-\psi)\alpha\Lambda_h)}{k_1 k_2} \\ 0 & 0 & 0 \\ 0 & 0 & \frac{\beta_b\Lambda_b}{\mu_b} \end{pmatrix}$$

and

$$V = \begin{pmatrix} k_3 & 0 & 0 \\ -\rho & k_4 & 0 \\ 0 & 0 & \mu_b \end{pmatrix},$$

where $k_1 = (\alpha + \mu_h)$, $k_2 = (\sigma + \mu_h)$, $k_3 = (\rho + \tau_1 + \mu_h)$, $k_4 = (\tau_2 + \mu_h)$. It follows that the spectral radius of FV^{-1} is the effective reproduction number given by

$$\mathcal{R}_e = \max\{\mathcal{R}_h,\ \mathcal{R}_h\}, \tag{3.5}$$

where

$$\mathcal{R}_h = \left\{ \frac{(k_2 + (1-\psi)\alpha)(\Lambda_h\beta_h k_4 + \theta\rho\beta_h\Lambda_h)}{k_1 k_2 k_3 k_4} \right\},$$

and

$$\mathcal{R}_b = \frac{\beta_b\Lambda_b}{\mu_b^2}.$$

Then, the following local stability result due to Theorem 2 of [24], holds.

Lemma 3.1. *The influenza-free steady state, represented by $\mathcal{E}_0$, of the influenza model* (2.11) *is locally asymptotically stable if $\mathcal{R}_e < 1$, and unstable if $\mathcal{R}_e > 1$.*

It is worth mentioning that, the effective reproduction number, $\mathcal{R}_e$, of the influenza model (2.11) measures the spread potential of influenza when a typical infectious individual is introduced into a susceptible and vaccinated populations [25, 26]. Epidemiologically, Lemma 3.1 implies that elimination of influenza virus infection is achievable in the population provided the initial sizes of the active influenza cases can be brought to the basin of attraction of the influenza-free steady state, such that $\mathcal{R}_e < 1$.

3.2.2. *Endemic equilibrium (EE).* Let the influenza-present (endemic) steady state of the model system (2.11) be delineated by $\mathcal{E}^{**} = (S_u^{**}, S_i^{**}, V^{**}, I_{1h}^{**}, I_{2h}^{**}, R^{**}, S_b^{**}, I_b^{**})$ and the forces of infection at steady states be represented by $\lambda_h^{**} = \beta_h(I_{1h}^{**} + I_b^{**} + \theta I_{2h}^{**})$ and $\lambda_b^{**} = \beta_b I_b^{**}$. Solving the influenza model (2.11) simultaneously in terms of λ_h^{**} and λ_b^{**} gives

$$\begin{cases} S_u^{**} = \dfrac{\Lambda_h}{\lambda_h^{**} + k_1}, \\ S_i^{**} = \dfrac{\alpha\Lambda_h}{(\lambda_h^{**} + k_1)[(1-\psi)\lambda_h^{**} + k_2]}, \\ V^{**} = \dfrac{\sigma\alpha\Lambda_h}{\mu_h(\lambda_h^{**} + k_1)[(1-\psi)\lambda_h^{**} + k_2]}, \\ I_{1h}^{**} = \dfrac{\lambda_h^{**}\Lambda_h[(1-\psi)(\lambda_h^{**} + \alpha) + k_3]}{k_3(\lambda_h^{**} + k_1)[(1-\psi)\lambda_h^{**} + k_2]}, \\ I_{2h}^{**} = \dfrac{\lambda_h^{**}\Lambda_h[(1-\psi)(\rho\lambda_h^{**} + \alpha) + \rho k_3]}{k_3k_4(\lambda_h^{**} + k_1)[(1-\psi)\lambda_h^{**} + k_2]}, \\ R^{**} = \dfrac{\lambda_h^{**}\Lambda_h([(1-\psi)(\lambda_h^{**} + 1) + k_2])(\tau_1k_4 + \tau_2\rho)}{\mu_h k_3k_4(\lambda_h^{**} + k_1)[(1-\psi)\lambda_h^{**} + k_2]}, \\ S_b^{**} = \dfrac{\Lambda_b}{\lambda_b^{**} + \mu_b}, \\ I_b^{**} = \dfrac{\lambda_b^{**}\Lambda_b}{\mu_b(\lambda_b^{**} + \mu_b)}. \end{cases}$$

It follows, using I_{1h}^{**}, I_b^{**}, and I_{2h}^{**} in λ_h^{**}, that the non-trivial equilibria of the influenza model (2.11) satisfies the cubic polynomial

$$a_1(\lambda^{**})^3 + a_2(\lambda^{**})^2 + a_3\lambda^{**} + a_4 = 0, \tag{3.6}$$

where the coefficients a_1, a_2, a_3, and a_4 are given as follows

$$\begin{aligned} a_1 &= \mu_b k_3 k_4(1-\psi), \\ a_2 &= \mu_b k_1 k_3 k_4(k_2 + (1-\psi)) - \Lambda_h\beta_h\mu_b(k_4 + \theta\rho)(1-\psi) + \beta_h k_3 k_4 \mu_b^2(1-\mathcal{R}_b)(1-\psi), \\ a_3 &= \tfrac{\mu_b}{k_1k_2k_3k_4}(1-\mathcal{R}_h) + k_3k_4\mu_b^2(1-\mathcal{R}_b)(k_2 + k_1(1-\psi)), \\ a_4 &= k_1k_2k_3k_4\mu_b^2(1-\mathcal{R}_b). \end{aligned}$$

It is imperative to mention that the cubic polynomial (3.6) demonstrates the likelihood of multiple endemic steady states for the influenza model. It can be seen that the coefficient a_1 of the cubic polynomial remains positive with non-negative parameters, while coefficients a_3 and a_4 remain negative whenever $\mathcal{R}_h > 1$ and $\mathcal{R}_b > 1$. Then, by Descartes' rule of signs [27, 28], the polynomial will always have a positive root, regardless of the signs of the coefficient a_2, whenever $\mathcal{R}_h > 1$ and $\mathcal{R}_b > 1$. Hence, the avian influenza model (2.11) has a unique influenza-present steady state at the threshold $\mathcal{R}_e = \max\{\mathcal{R}_h, \mathcal{R}_b\} > 1$.

3.3. **Global asymptotic dynamics of influenza model.** This subsection seeks to explore the behavior of the dynamics of the avian influenza model (2.11) as its solution tends to the influenza-free and influenza-present equilibria.

3.3.1. *Global stability of influenza-free equilibrium.* Using the approach in [29–31], the system (2.11) can be re-written as

$$\begin{aligned} \frac{dX}{dt} &= F(X, Z), \\ \frac{dZ}{dt} &= G(X, Z),\ G(X, 0) = 0, \end{aligned} \tag{3.7}$$

where $X \in \mathbb{R}^5_+$ and $Z \in \mathbb{R}^3_+$. It is worth mentioning that $X = (S_u, S_i, V, R, S_b)$ forms the component of the uninfected populations, while $Z = (I_{1h}, I_{2h}, I_b)$ represents the infected populations. The avian influenza-free equilibrium of the model system (2.11) is delineated by $\mathcal{E}_0 = (X^0, 0)$, such that its global asymptotic stability is established provided the following properties are met.

(P1): For $\dfrac{dX}{dt} = F(X, 0)$, X^* is globally asymptotically stable,
(P2): $G(X, Z) = AZ - \widehat{G}(X, Z)$, $\widehat{G}(X, Z) \geq 0$, for $(X, Z) \in \mathbb{R}^8_+$,

where $A = \partial G/\partial Z$ is a Metzler matrix with non-negative off diagonal elements evaluated at $(X^0, 0)$.

Theorem 3.2. *The influenza-free equilibrium point, $\mathcal{E}_0 = (X^0, 0)$, of the avian influenza model* (2.11) *is globally-asymptotically stable if the conditions (P1) and (P2) are satisfied.*

Proof. The functions $F(X, Z)$ and $G(X, Z)$ are obtained from (3.7) as follows:

$$F(X, Z) = \begin{pmatrix} \Lambda_h - \beta_h \left(I_{1h} + I_b + \theta I_{2h}\right) S_u - (\alpha + \mu_h) S_u \\ \alpha Su - (1 - \psi)\beta_h \left(I_{1h} + I_b + \theta I_{2h}\right) S_i - (\sigma + \mu_h) S_i \\ \sigma S_i - \mu_h V \\ \tau_1 I_{1h} + \tau_2 I_{2h} - \mu_h R \\ \Lambda_b - \beta_b S_b I_b - \mu_b S_b \end{pmatrix}, \tag{3.8}$$

and

$$G(X, Z) = \begin{pmatrix} \beta_h \left(I_{1h} + I_b + \theta I_{2h}\right) \left(S_u + (1 - \psi) S_i\right) - (\rho + \tau_1 + \mu_h) I_{1h} \\ \rho I_{1h} - (\tau_2 + \mu_h) I_{2h} \\ \beta_b S_b I_b - \mu_b I_b \end{pmatrix}. \tag{3.9}$$

Then, $dX/dt = F(X,0)$ implies that

$$\begin{aligned}
\frac{dS_u}{dt} &= \Lambda_h - (\alpha + \mu_h)S_u, \\
\frac{dS_i}{dt} &= \alpha Su - (\sigma + \mu_h)S_i, \\
\frac{dV}{dt} &= \sigma S_i - \mu_h V, \\
\frac{dR}{dt} &= -\mu_h R, \\
\frac{dS_b}{dt} &= \Lambda_b - \mu_b S_b.
\end{aligned} \tag{3.10}$$

Now, solving system (3.10) simultaneously yields

$$S_u(t) = \frac{\Lambda_h}{(\alpha+\mu_h)} + \left(S_u(0) - \frac{\Lambda_h}{\alpha+\mu_h}\right)e^{-(\alpha+\mu_h)t},$$

$$S_i(t) = \frac{\alpha\Lambda_h}{(\sigma+\mu_h)(\alpha+\mu_h)} + \frac{\alpha}{(\sigma-\alpha)}(e^{-(\alpha+\mu_h)t} - e^{-(\sigma+\mu_h)t})\left(S_u(0) - \frac{\Lambda_h}{\alpha+\mu_h}\right)$$

$$+\left(S_i(0) - \frac{\alpha\Lambda_h}{(\sigma+\mu_h)(\alpha+\mu_h)}\right)e^{-(\sigma+\mu_h)t},$$

$$V(t) = \frac{\sigma\alpha\Lambda_h}{\mu_h(\sigma+\mu_h)(\alpha+\mu_h)} + \frac{\sigma\alpha}{\mu_h(\sigma-\alpha)}(e^{-(\alpha+\mu_h)t} - e^{-(\sigma+\mu_h)t})\left(S_u(0) - \frac{\Lambda_h}{\alpha+\mu_h}\right) \tag{3.11}$$

$$+\left(V(0) - \frac{\Lambda_h}{(\alpha+\mu_h)}\right)e^{-\mu_h t} + \left(S_i(0) - \frac{\Lambda_h}{\alpha+\mu_h}\right)(e^{-\mu_h t} - e^{-(\sigma+\mu_h)t}),$$

$$R(t) = R(0)e^{-\mu_h t},$$

$$S_b(t) = \frac{\Lambda_b}{\mu_b} + \left(S_b(0) - \frac{\Lambda_b}{\mu_b}\right)e^{-\mu_b t}.$$

Without minding the sizes of $(S_u(0), S_i(0), V(0), R(0), S_b(0))$ as $t \to \infty$, it is perceived that $(S_u, S_i, V, R, S_b) \to (S_u^0, S_i^0, V^0, R^0, S_b^0)$. Therefore, X^0 is globally asymptotically stable, satisfying condition (P1). Furthermore, an M-matrix with non-negative off diagonal entries is given by

$$A = \begin{pmatrix} \beta_h(S_u^0 + (1-\psi)S_i^0) - k_3 & \theta\beta_h(S_u^0 + (1-\psi)S_i^0) & \beta_h(S_u^0 + (1-\psi)S_i^0) \\ \rho & -(\tau_2 + \mu_h) & 0 \\ 0 & 0 & (\beta_b S_b^0 - \mu_b) \end{pmatrix}. \tag{3.12}$$

Then, $\widehat{G}(X,Z) = AZ - G(X,Z)$ yields

$$\widehat{G}(X,Z) = \begin{pmatrix} \beta_h(I_{1h}+I_{2h}+I_b)(S_u^0 - S_u) + (1-\psi)\beta_h\left(I_{1h}+I_b+\theta I_{2h}\right)\left(S_i^0 - S_i\right) \\ 0 \\ \beta_b I_b\left(S_b^0 - S_b\right) \end{pmatrix}. \tag{3.13}$$

It is apparent that $\widehat{G}(X,Z) \geq 0$, since $0 \leq S_u \leq S_u^0$, $0 \leq S_i \leq S_i^0$, and $0 \leq S_b \leq S_b^0$. Thus, condition (P2) is preserved. Hence, it is sufficient to conclude that the influenza-free equilibrium, $\mathcal{E}_0$, of the influenza model (2.11) is globally-asymptotically stable. This completes the proof. □

Consequently, from the epidemiological viewpoint, Theorem 3.2 implies that, avian influenza virus infection could be eliminated from the population regardless of the initial numbers of non-isolated and isolated infectious humans and infectious birds if $\mathcal{R}_e < 1$. See Figure 2 for pictorial representation of the convergence of trajectories of non-isolated and isolated infectious humans and infectious birds to the influenza-free equilibrium point asymptotically at various initial sizes. This practically implies that elimination of influenza is achievable in the population.

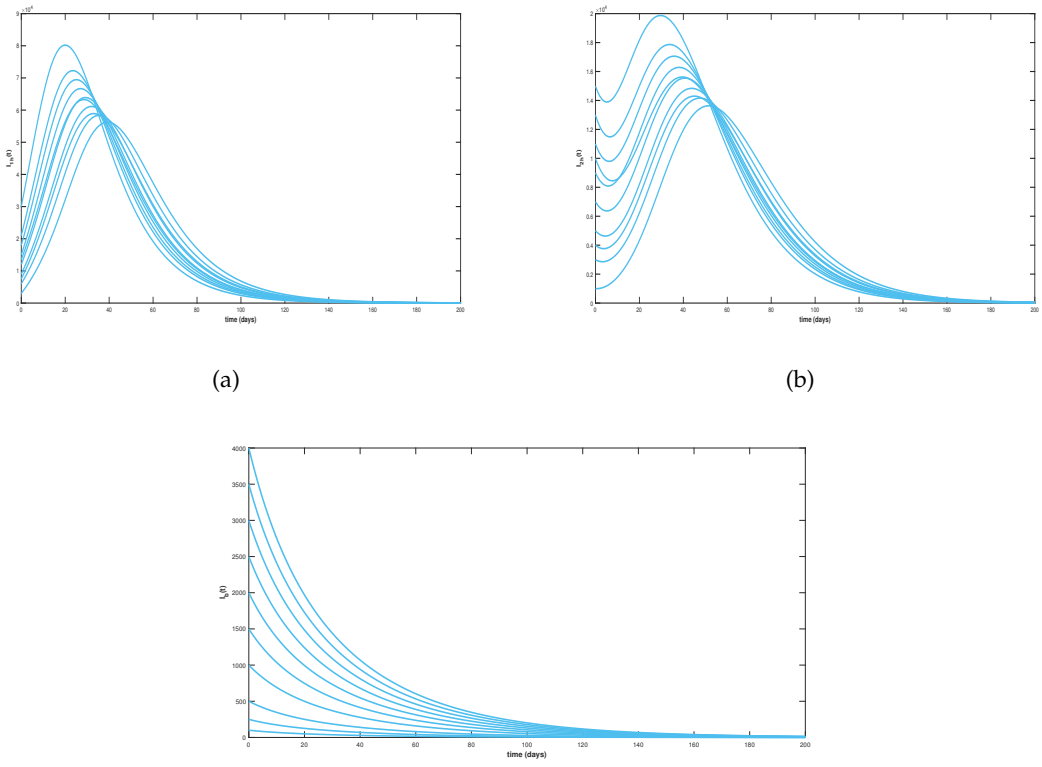

(a) (b)

(c)

FIGURE 2. Convergence of trajectories of active infectious humans (isolated and non-isolated) and infectious birds at different values of initial data. Parameter values given in Table 3 are used, so that $\mathcal{R}_h = 0.2033 < 1$ and $\mathcal{R}_b = 0.5556 < 1$.

3.3.2. *Global stability of endemic equilibrium.*

Theorem 3.3. *The unique influenza-present (endemic) equilibrium point, $\mathcal{E}^{**}$, of the avian influenza model* (2.11) *is globally asymptotically stable if the effective reproduction number, $\mathcal{R}_e$, is more than unity.*

Proof. Consider a quadratic Lyapunov function defined by (see, [31,32])

$$\begin{aligned}\mathfrak{L} &= \tfrac{1}{2}\Big[(S_u - S_u^{**}) + (S_i - S_i^{**}) + (V - V^{**}) + (I_{1h} - I_{1h}^{**}) + (I_{2h} - I_{2h}^{**}) + (R - R^{**})\Big]^2 \\ &\quad + \tfrac{1}{2}\Big[(S_b - S_b^{**}) + (I_b - I_b^{**})\Big]^2.\end{aligned} \tag{3.14}$$

Taking the time derivative of the Lyapunov function (3.14) gives

$$\begin{aligned}\dot{\mathfrak{L}} &= [(S_u - S_u^{**}) + (S_i - S_i^{**}) + (V - V^{**}) + (I_{1h} - I_{1h}^{**}) + (I_{2h} - I_{2h}^{**}) + (R - R^{**})] \\ &\quad \times \frac{d}{dt}(S_u + S_i + V + I_{1h} + I_{2h} + R) + [(S_b - S_b^{**}) + (I_b - I_b^{**})] \times \frac{d}{dt}(S_b + I_b), \\ &= [(S_u - S_u^{**}) + (S_i - S_i^{**}) + (V - V^{**}) + (I_{1h} - I_{1h}^{**}) + (I_{2h} - I_{2h}^{**}) + (R - R^{**})] \\ &\quad \times (\Lambda_h - \mu(S_u + S_i + V + I_{1h} + I_{2h} + R)) + [(S_b - S_b^{**}) + (I_b - I_b^{**})] \\ &\quad \times (\Lambda_b - \mu_b(S_b + I_b)),\end{aligned}$$

$$\begin{aligned}\dot{\mathfrak{L}} &\leq -\mu_h[(S_u - S_u^{**}) + (S_i - S_i^{**}) + (V - V^{**}) + (I_{1h} - I_{1h}^{**}) + (I_{2h} - I_{2h}^{**}) + (R - R^{**})] \\ &\quad \times \left((S_u + S_i + V + I_{1h} + I_{2h} + R) - \frac{\Lambda_h}{\mu_h}\right) - \mu_b[(S_b - S_b^{**}) + (I_b - I_b^{**})] \\ &\quad \times \left((S_b + I_b) - \frac{\Lambda_b}{\mu_b}\right).\end{aligned} \tag{3.15}$$

Now, using the limiting values $N_h^{**} = \Lambda_h/\mu_h$ and $N_b^{**} = \Lambda_b/\mu_b$, respectively, it follows that (3.15) becomes

$$\begin{aligned}\dot{\mathfrak{L}} &\leq -\mu_h[(S_u - S_u^{**}) + (S_i - S_i^{**}) + (V - V^{**}) + (I_{1h} - I_{1h}^{**}) + (I_{2h} - I_{2h}^{**}) + (R - R^{**})] \\ &\quad \times [(S_u + S_i + V + I_{1h} + I_{2h} + R) - (S_u^{**} + S_i^{**} + V^{**} + I_{1h}^{**} + I_{2h}^{**} + R^{**})] \\ &\quad -\mu_b\Big[(S_b - S_b^{**}) + (I_b - I_b^{**})\Big] \times [(S_b + I_b) - (S_b^{**} + I_b^{**})], \\ &= -\mu_h\Big[(S_u - S_u^{**}) + (S_i - S_i^{**}) + (V - V^{**}) + (I_{1h} - I_{1h}^{**}) + (I_{2h} - I_{2h}^{**}) + (R - R^{**})\Big]^2 \\ &\quad -\mu_b\Big[(S_b - S_b^{**}) + (I_b - I_b^{**})\Big]^2.\end{aligned} \tag{3.16}$$

Clearly, the continuously differentiable function $\mathfrak{L}$ defined in (3.14) is a Lyapunov function since its time-derivative is negative semi-definite, implying that, $\dot{\mathfrak{L}} \leq 0$. Moreover, $\dot{\mathfrak{L}} = 0$, if $S_u = S_u^{**}, S_i = S_i^{**}, V = V^{**}, I_{1h} = I_{1h}^{**}, I_{2h} = I_{2h}^{**}, R = R^{**}, S_b = S_b^{**}$, and $I_b = I_b^{**}$. Then, the largest invariance set for which $\dot{\mathfrak{L}} = 0$ is the singleton $\{\mathcal{E}^{**}\}$. It therefore follows by invoking the spirit of LaSalle's invariance principle [33], that the influenza-present equilibrium point, $\mathcal{E}^{**}$, is globally asymptotically stable. This wraps up the proof. □

The global asymptotic stability of endemic equilibrium, $\mathcal{E}^{**}$, presented in Theorem (3.3) indicates that the spread of influenza infection will persist in the population whenever the associated effective reproduction number, $\mathcal{R}_e$, transcends unity, notwithstanding the initial sizes of the isolated and non-isolated human and bird populations of the system (2.11). This result is quantitatively buttressed as presented in Figure 3.

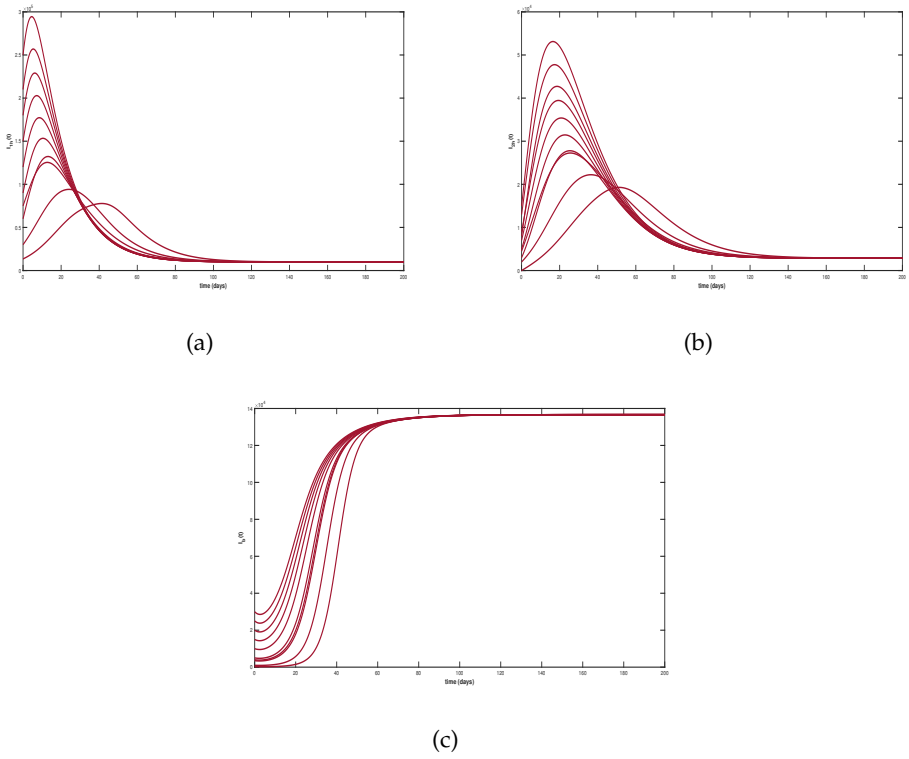

(a) (b)

(c)

FIGURE 3. Convergence of trajectories of infectious (isolated and non-isolated) humans and infectious birds at different values of initial data. Parameter values given in Table 3 are used except that $\Lambda_h = 700$ and $\Lambda_b = 10000$, so that $\mathcal{R}_h = 4.7437 > 1$ and $\mathcal{R}_b = 5.556 > 1$.

4. Analysis of Optimal Control Problem

In an attempt to fight against the evolution of avian influenza transmission in the population, an optimal control framework is designed such that the constant parameter, ψ, which measures

TABLE 3. Description and values of parameters of the model.

Parameters	Values	References
Λ_h	30	[8,38]
Λ_b	1000	[8,38]
β_h	6×10^{-7}	[8,38]
β_b	2×10^{-6}	[8,38]
μ_h	$\frac{1}{70\times365}$	[8,38]
μ_b	0.06	Assumed
α	0.002	Assumed
τ_1	0.05	[8,38]
θ	0.55	Assumed
ψ	0.007	Assumed
τ_2	0.07	Assumed
σ	0.005	Assumed
ρ	0.02	Assumed

the rate of adherence to precautionary education on influenza becomes a time-dependent control, $0 \le \psi(t) \le 1$, while the constant vaccination rate, σ, becomes a time-dependent control $0 \le \sigma(t) \le 1$. Other two time-dependent control interventions including, anti-viral treatment, $0 \le U_h(t) \le 1$, and culling (removal of sick or infected birds from the flock), $0 \le U_b(t) \le 1$, are incorporated. Consequently, the autonomous system of equations describing the transmission dynamics of avian influenza given in (2.11) is transformed to non-autonomous system given by

$$\begin{aligned}
\frac{dS_u}{dt} &= \Lambda_h - \beta_h\left(I_{1h}+I_b+\theta I_{2h}\right)S_u - (\alpha+\mu_h)S_u,\\
\frac{dS_i}{dt} &= \alpha Su - (1-\psi(t))\beta_h\left(I_{1h}+I_b+\theta I_{2h}\right)S_i - (\sigma(t)+\mu_h)S_i,\\
\frac{dV}{dt} &= \sigma(t)S_i - \mu_h V,\\
\frac{dI_{1h}}{dt} &= \beta_h\left(I_{1h}+I_b+\theta I_{2h}\right)S_u + (1-\psi(t))\beta_h\left(I_{1h}+I_b+\theta I_{2h}\right)S_i - (\rho+\tau_1+\mu_h)I_{1h},\\
\frac{dI_{2h}}{dt} &= \rho I_{1h} - (\tau_2+c_0U_h(t)+\mu_h)I_{2h},\\
\frac{dR}{dt} &= \tau_1 I_{1h} + (\tau_2+c_0U_h(t))I_{2h} - \mu_h R,\\
\frac{dS_b}{dt} &= \Lambda_b - \beta_b S_b I_b - \mu_b S_b,\\
\frac{dI_b}{dt} &= \beta_b S_b I_b - \mu_b I_b - U_b(t)I_b.
\end{aligned} \tag{4.1}$$

The control dynamical system (4.1) is analysed via the optimal control theory using the well-known Pontryagin's Maximum Principle [34–37]. Of particular interest is to find an optimal solution for problem of minimizing the populations of isolated and non-isolated infectious humans and birds, while minimizing the associated cost of the intervention implementation. Thus, the performance index, $\mathfrak{J}$, needed to execute this over a fixed time window $[0, T_f]$ is given by

$$\mathfrak{J} = \int_0^{T_f} \Big(A_1 I_{1h} + A_2 I_{2h} + A_3 I_b + \frac{1}{2}(B_1\psi^2(t) + B_2\sigma^2(t) + B_3 U_h^2(t) + B_4 U_b^2(t)) \Big) dt, \tag{4.2}$$

where, A_i, $(i = 1, 2, 3)$ are the positive weight constants for non-isolated infectious human, isolated infectious human, and infectious birds, respectively. B_i, $(i = 1, 2, 3, 4)$, are the balancing weight constants for the control interventions $\psi(t)$, $\sigma(t)$, $U_h(t)$ and $U_b(t)$, respectively. The costs of implementing each of the control interventions are, respectively, represented by $1/2B_1\psi^2(t)$, $1/2B_2\sigma^2(t)$, $1/2B_3U_h^2(t)$, and $1/2B_4U_b^2(t)$. It should be mentioned that the cost functions are in quadratic form as used in the previous studies on optimal control in the literature [38–41]. As a consequence of the foregoing, it becomes essential to seek an optimal control quadruple, $(\psi^*, \sigma^*, U_h^*, U_b^*)$ such that

$$\mathfrak{J}(\psi^*, \sigma^*, U_h^*, U_b^*) = \min\{\mathfrak{J}(\psi, \sigma, U_h, U_b) : (\psi, \sigma, U_h, U_b) \in \mathbb{U}\}, \tag{4.3}$$

subject to the state system (4.1), where the control set is given by a Lebesgue measurable $\mathbb{U} = \{(\psi(t), \sigma(t), U_h(t), U_b(t)) : 0 \leq \psi(t), \sigma(t), U_h(t), U_b(t) \leq 1, \text{ and } t \in [0, T_f]\}$.

4.1. **Characterization of Optimal Control.** The Hamiltonian, $\mathbb{H}$, needed for the characterization of the optimal control quadruple $(\psi^*, \sigma^*, U_h^*, U_b^*)$ for the minimization problem (4.3) is given by

$$\begin{aligned}
\mathbb{H} = \; & A_1 I_{1h} + A_2 I_{2h} + A_3 I_b + 1/2(B_1\psi^2(t) + B_2\sigma^2(t) + B_3 U_h^2(t) + B_4 U_b^2(t)) \\
& + \lambda_1(\Lambda_h - \beta_h (I_{1h} + I_b + \theta I_{2h}) S_u - (\alpha + \mu_h) S_u) \\
& + \lambda_2(\alpha S u - (1 - \psi(t))\beta_h (I_{1h} + I_b + \theta I_{2h}) S_i - (\sigma(t) + \mu_h) S_i,) \\
& + \lambda_3(\sigma(t) S_i - \mu_h V) \\
& + \lambda_4(\beta_h (I_{1h} + I_b + \theta I_{2h}) S_u + (1 - \psi(t))\beta_h (I_{1h} + I_b + \theta I_{2h}) S_i - (\rho + \tau_1 + \mu_h) I_{1h}) \\
& + \lambda_5(\rho I_{1h} - (\tau_2 + c_0 U_h(t) + \mu_h) I_{2h}) \\
& + \lambda_6(\tau_1 I_{1h} + (\tau_2 + c_0 U_h(t)) I_{2h} - \mu_h R) \\
& + \lambda_7(\Lambda_b - \beta_b S_b I_b - \mu_b S_b), \\
& + \lambda_8(\beta_b S_b I_b - \mu_b I_b - U_b(t) I_b),
\end{aligned} \tag{4.4}$$

where λ_i, $i = 1, 2, ..., 8$, are called adjoint variables corresponding to the state variables S_u, S_i, V, I_{1h}, I_{2h}, R, S_b, and I_b of the avian influenza system (4.1). Then, the following existence result is claimed.

Theorem 4.1. *Given an optimal control* $(\psi^*(t), \sigma^*(t), U_h^*(t), U_b^*(t))$ *and solutions of the corresponding state system* (4.1) *satisfying* (4.3)*, then there exist adjoint variables* λ_1, λ_2, λ_3, λ_4, λ_5, λ_6, λ_7, *and* λ_8 *satisfying the adjoint system given by*

$$\begin{aligned}
\frac{d\lambda_1}{dt} &= \beta_h \left(I_{1h} + I_b + \theta I_{2h}\right)(\lambda_1 - \lambda_4) + \alpha(\lambda_1 - \lambda_2) + \mu_h \lambda_1 \\
\frac{d\lambda_2}{dt} &= (1 - \psi(t))\beta_h \left(I_{1h} + I_b + \theta I_{2h}\right)(\lambda_2 - \lambda_4) + \sigma(t)(\lambda_2 - \lambda_3) + \mu_h \lambda_2 \\
\frac{d\lambda_3}{dt} &= \mu_h \lambda_3 \\
\frac{d\lambda_4}{dt} &= \beta_h S_u(\lambda_1 - \lambda_4) + (1 - \psi(t))\beta_h S_i(\lambda_2 - \lambda_4) + \rho(\lambda_4 - \lambda_5) + \tau_1(\lambda_4 - \lambda_6) + \mu_h \lambda_4 - A_1 \\
\frac{d\lambda_5}{dt} &= \beta_h \theta S_u(\lambda_1 - \lambda_4) + (1 - \psi(t))\beta_h \theta S_i(\lambda_2 - \lambda_4) + (\tau_2 + c_0 U_h(t))(\lambda_5 - \lambda_6) + \mu_h \lambda_5 - A_2 \\
\frac{d\lambda_6}{dt} &= \mu_h \lambda_6 \\
\frac{d\lambda_7}{dt} &= \beta_b I_b(\lambda_7 - \lambda_8) + \mu_b \lambda_7 \\
\frac{d\lambda_8}{dt} &= \beta_h S_u(\lambda_1 - \lambda_4) + (1 - \psi(t))\beta_h S_i(\lambda_2 - \lambda_4) + \beta_b S_b(\lambda_7 - \lambda_8) + (\mu_b + U_b(t))\lambda_8,
\end{aligned} \tag{4.5}$$

with transversality conditions

$$\lambda_i(T_f) = 0, i = 1, 2, ..., 8, \tag{4.6}$$

and control characterizations

$$\begin{aligned}
\psi(t)^* &= \min\left\{\max\left\{0, \frac{\beta_h \left(I_{1h} + I_b + \theta I_{2h}\right) S_i(\lambda_4 - \lambda_2)}{B_1}\right\}, 1\right\}, \\
\sigma(t)^* &= \min\left\{\max\left\{0, \frac{S_i(\lambda_2 - \lambda_3)}{B_2}\right\}, 1\right\}, \\
U_h(t)^* &= \min\left\{\max\left\{0, \frac{c_0 I_{2h}(\lambda_5 - \lambda_6)}{B_3}\right\}, 1\right\}, \\
U_b(t)^* &= \min\left\{\max\left\{0, \frac{\lambda_8 I_b}{B_4}\right\}, 1\right\}.
\end{aligned} \tag{4.7}$$

Proof. The adjoint equations in (4.5) are generated by partially differentiating the Hamiltonian (4.4) with respect to the corresponding state variables as follows

$$\frac{d\lambda_1}{dt} = -\frac{\partial \mathbb{H}}{\partial S_u},\ \lambda_1(T_f) = 0;\ \frac{d\lambda_2}{dt} = -\frac{\partial \mathbb{H}}{\partial S_i},\ \lambda_2(T_f) = 0;\ \frac{d\lambda_3}{dt} = -\frac{\partial \mathbb{H}}{\partial V},\ \lambda_3(T_f) = 0;$$

$$\frac{d\lambda_4}{dt} = -\frac{\partial \mathbb{H}}{\partial I_{1h}},\ \lambda_4(T_f) = 0;\ \frac{d\lambda_5}{dt} = -\frac{\partial \mathbb{H}}{\partial I_{2h}},\ \lambda_5(T_f) = 0;\ \frac{d\lambda_6}{dt} = -\frac{\partial \mathbb{H}}{\partial R},\ \lambda_6(T_f) = 0;$$

$$\frac{d\lambda_7}{dt} = -\frac{\partial \mathbb{H}}{\partial S_b},\ \lambda_7(T_f) = 0;\ \frac{d\lambda_8}{dt} = -\frac{\partial \mathbb{H}}{\partial I_b},\ \lambda_8(T_f) = 0.$$

In addition, the optimal control characterization (4.7) is derived by solving for $\psi^*(t)$, $\sigma^*(t)$, $U_h^*(t)$, and $U_b^*(t)$, respectively, from the optimality conditions

$$\begin{aligned}
\frac{\partial \mathbb{H}}{\partial \psi} &= B_1\psi^* + \beta_h\left(I_{1h} + I_b + \theta I_{2h}\right) S_i(\lambda_2 - \lambda_4) = 0,\\
\frac{\partial \mathbb{H}}{\partial \sigma} &= B_2\sigma^* + S_i(\lambda_3 - \lambda_2) = 0,\\
\frac{\partial \mathbb{H}}{\partial U_h} &= B_3U_h^* + c_0I_{2h}(\lambda_6 - \lambda_5) = 0,\\
\frac{\partial \mathbb{H}}{\partial U_b} &= B_4U_b^* - \lambda_8I_b = 0.
\end{aligned} \tag{4.8}$$

It therefore follows by invoking the spirit of standard arguments involving the bounds on controls [42, 43] that

$$\psi^* = \begin{cases} \Psi_1^*, & \text{for } 0 < \Psi_1^* < 1\\ 0, & \text{for } \Psi_1^* \le 0\\ 1, & \text{for } \Psi_1^* \ge 1, \end{cases} \quad \sigma^* = \begin{cases} \Psi_2^*, & \text{for } 0 < \Psi_2^* < 1\\ 0, & \text{for } \Psi_2^* \le 0\\ 1, & \text{for } \Psi_2^* \ge 1, \end{cases} \quad U_h^* = \begin{cases} \Psi_3^*, & \text{for } 0 < \Psi_3^* < 1\\ 0, & \text{for } \Psi_3^* \le 0\\ 1, & \text{for } \Psi_3^* \ge 1, \end{cases}$$

and

$$U_b^* = \begin{cases} \Psi_4^*, & \text{for } 0 < \Psi_4^* < 1\\ 0, & \text{for } \Psi_4^* \le 0\\ 1, & \text{for } \Psi_4^* \ge 1, \end{cases}$$

where

$$\begin{aligned}
\Psi_1^* &= \frac{\beta_h\left(I_{1h} + I_b + \theta I_{2h}\right) S_i(\lambda_4 - \lambda_2)}{B_1},\\
\Psi_2^* &= \frac{S_i(\lambda_2 - \lambda_3)}{B_2},\\
\Psi_3^* &= \frac{c_0I_{2h}(\lambda_5 - \lambda_6)}{B_3},\\
\Psi_4^* &= \frac{\lambda_8I_b}{B_4}.
\end{aligned}$$

This completes the proof. □

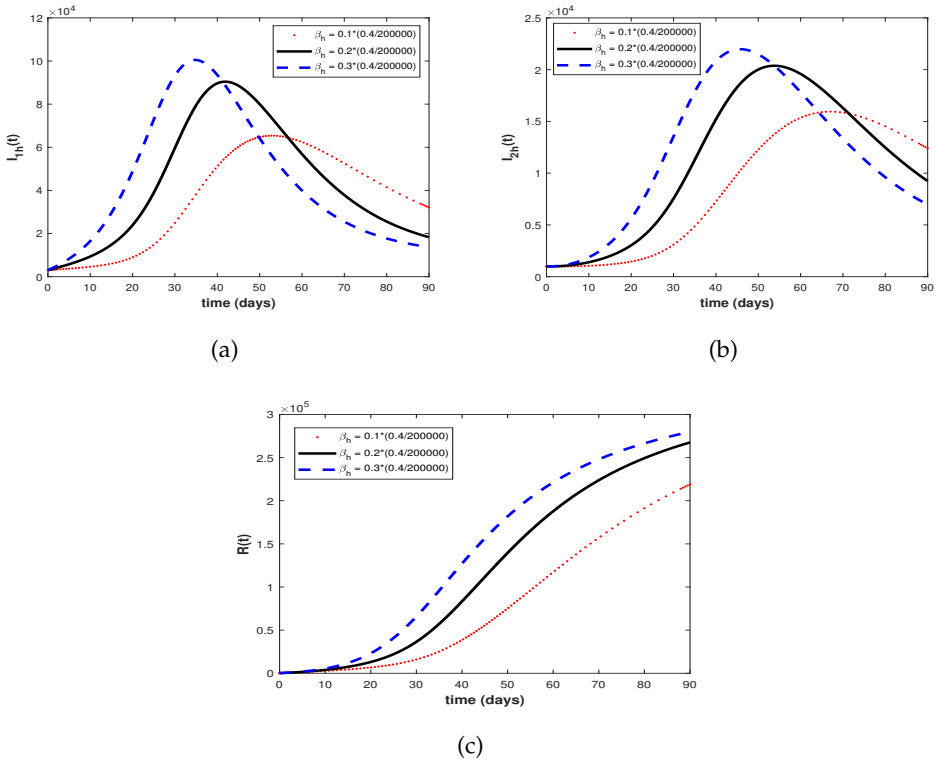

FIGURE 4. Effect of transmission probability of influenza infection in human on the evolution of non-isolated infectious, isolated infectious, and vaccinated classes.

4.2. **Simulations and discussions.** Here, numerical simulations are performed using the parameter values that correspond to the asymptotic stability of influenza-present equilibrium (see, Figure 3). The influence of certain epidemiological parameters of the model are examined. In particular, the effect of transmission probability, β_h, of infection in human is examined on the behavior of infectious (isolated and non-isolated) and recovered humans, accordingly as presented in Figure 4. It is observed that the magnitudes of non-isolated and isolated infectious humans and recovered population increase with time as transmission probability, β_h, increases, implying that influenza virus disease will be more prevalent if efforts are not put in place to hamper its transmission probability.

In a similar manner, Figure 5 showcases the effect of transmission probability, β_b, of infection in birds on the population of non-isolated and isolated infectious human and infectious birds. It can be seen that increase in transmission probability of influenza in birds increases the populations of non-isolated and isolated infectious humans and infectious birds. This suggests that, the elimination of influenza in the population will be difficult if its transmission in the avian population is not hindered. In another perspective, the influence of progression rate of uninformed susceptible to informed class on the populations of non-isolated and isolated infectious and vaccinated humans is depicted in Figure 6. It is easy to see that increase in the progression of individuals to the informed class as a result of public awareness campaign leads to a corresponding reduction in

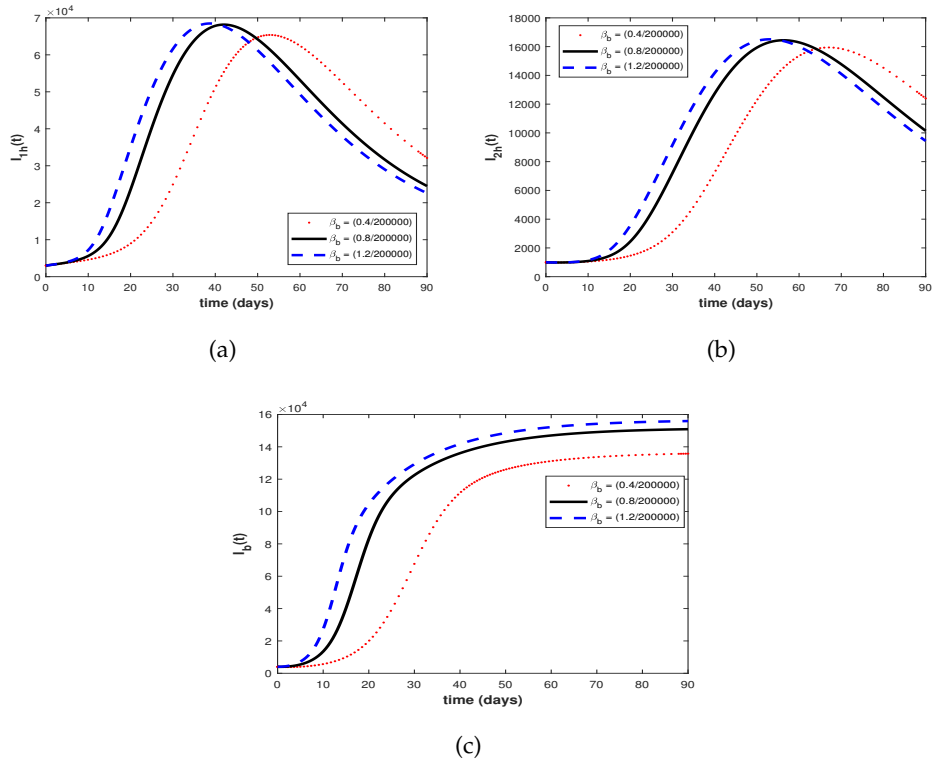

FIGURE 5. Effect of transmission probability of influenza infection in birds on the evolution of non-isolated and isolated infectious humans and infectious birds.

the populations of non-isolated and isolated infectious humans and vaccinated human. This corroborates the importance of disease awareness programs or public enlightenment campaigns in battling the spread of influenza in the population.

In another dimension in Figure 7, it is shown that the bird (avian) reproduction number, $\mathcal{R}_b$, increases from 0.5 to 4.0 as the recruitment rate into the bird population increases in the interval $1000 \leq \Lambda_b \leq 8000$, while increase in the value of natural mortality for birds in the interval $0.06 \leq \mu_b \leq 0.1$ leads to a corresponding decrease in the value of avian reproduction number from $\mathcal{R}_b = 4.0$ to $\mathcal{R}_b = 0.5$. Implying that while increase in recruitment of birds enhances the potential spread of infection from influenza-free state to influenza-present state, increase in deaths of birds slow down the spread strength of the infection. In a similar spirit, Figure 8 depicts how both modification parameter due to infectiousness in isolated infectious individuals, θ, and spontaneous recovery rate, τ_1, affect human reproduction number, $\mathcal{R}_h$. One sees that an increase in the value of θ increases the value of $\mathcal{R}_h$, thereby making the transmission of influenza infection more rampant in the population, while an increase in the value of τ_1 decreases the value of $\mathcal{R}_h$, suggesting elimination of influenza in the population if effective treatment is available.

Furthermore, simulations are performed to illustrate the significance of the four time-dependent optimal control functions in the non-autonomous avian influenza dynamic system. This is done by coupling the control dynamical system (4.1) and the adjoint system (4.5) with their corresponding

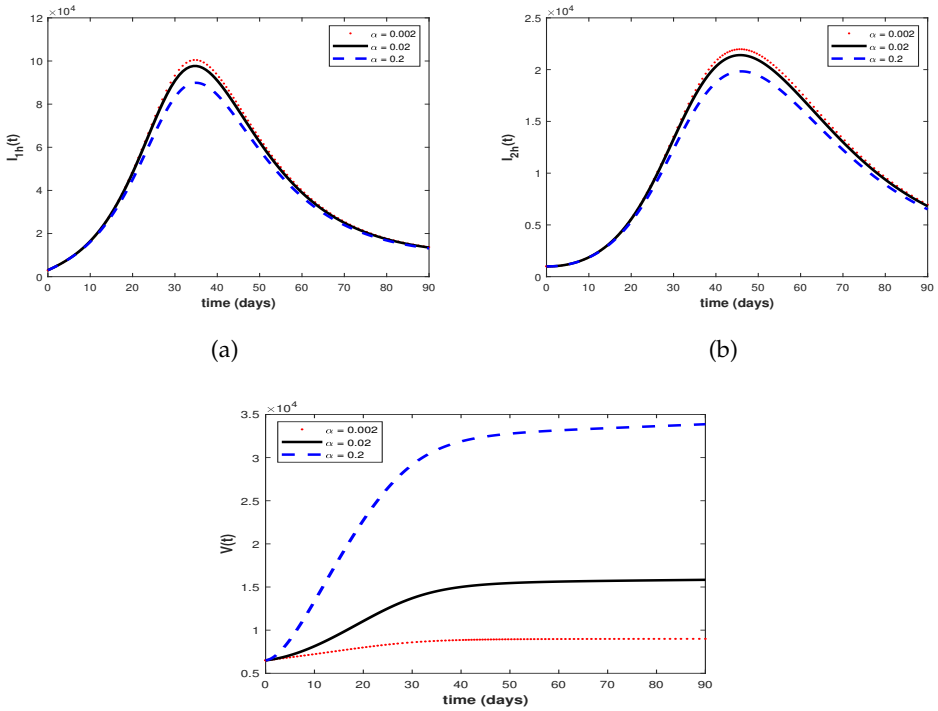

FIGURE 6. Effect of progression rate uninformed to informed susceptible on the evolution of non-isolated infectious, isolated infectious, and vaccinated classes.

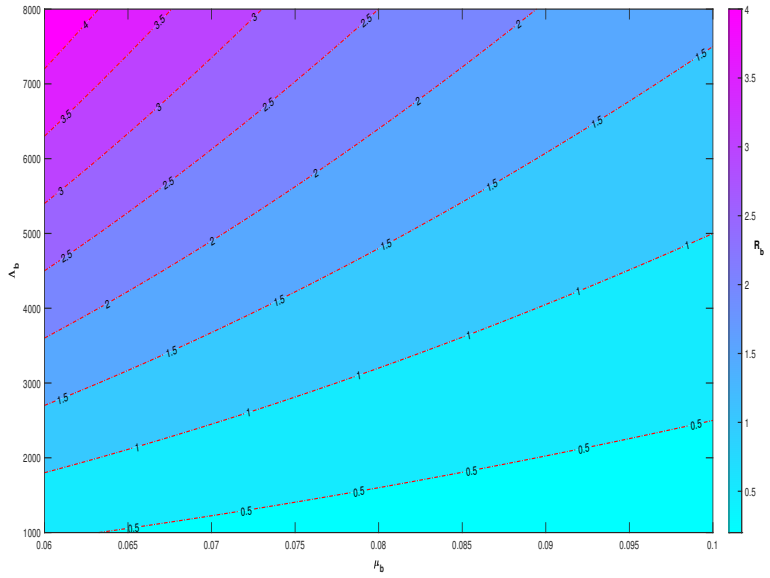

FIGURE 7. 2D contour plot showing the influence of birds recruitment rate and natural mortality rate on the avian reproduction number.

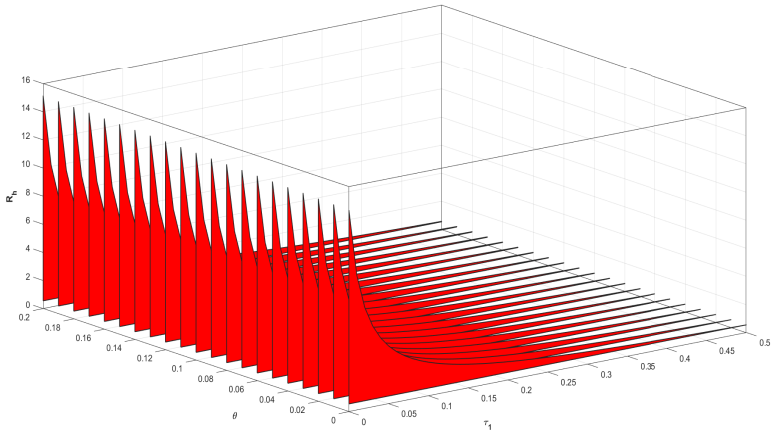

FIGURE 8. 3D plot showing the influence of modification parameter due to infectiousness in isolated infectious human and recovery rate due to treatment on the reproduction number of the avian influenza model.

initial (2.12) and transversality conditions (4.6) to form the optimality system. The so derived optimality system is solved using the forward-backward fourth order Runge-Kutta method following the iterative procedure made available in [44, 45]. The initial conditions of the state variables at time, $t = 0$, are taken as $S_u(0) = 231279, S_i(0) = 13000, V(0) = 6500, I_{1h}(0) = 3000, I_{2h}(0) = 1000, R(0) = 200, S_b(0) = 10000$ and $I_b(0) = 4000$. The time frame for the simulation of the optimality system is taken as $[0, 150]$ in days, while the values of the weight constants used in the performance index are chosen as $A_1 = 10$, $A_2 = 50$, $A_3 = 20$, $B_1 = 100$, $B_2 = 200$, $B_3 = 100$, $B_4 = 150$ and the rate constant $c_0 = 0.7$.

Consequently, the impact of combining any three of the control interventions are explored on the transmission dynamics of avian influenza model (4.1). The combined effects of the interventions $\psi(t)$, $\sigma(t)$ and $U_h(t)$ on the incidence of non-isolated and isolated infectious populations are depicted in Figure 9. It is observed that the sizes of non-isolated and isolated infectious classes reduce when control interventions are maximally implemented compared to the case when control interventions are not activated. It should be mentioned that a significant reduction is observed in the population of infectious individuals in isolation, suggesting that isolation plays a pertinent role in curtailing the dynamics of influenza in the population. The control profile displayed in Figure 9(c) implies that combination of control interventions $\psi(t)$, $\sigma(t)$ and $U_h(t)$ should be maintained at maximum (100%) within the first 55 days, 145 days, and 150 days, respectively, before gradually declining to zero at the final time.

In Figure 10, control interventions $\psi(t), \sigma(t)$ and $U_b(t)$ are combined to combat the transmission dynamics of avian influenza in the population. It is easy to see that the magnitude of non-isolated and isolated infectious human reduce significantly when control interventions are implemented. This epidemiologically implies that the combination of the three control interventions should be

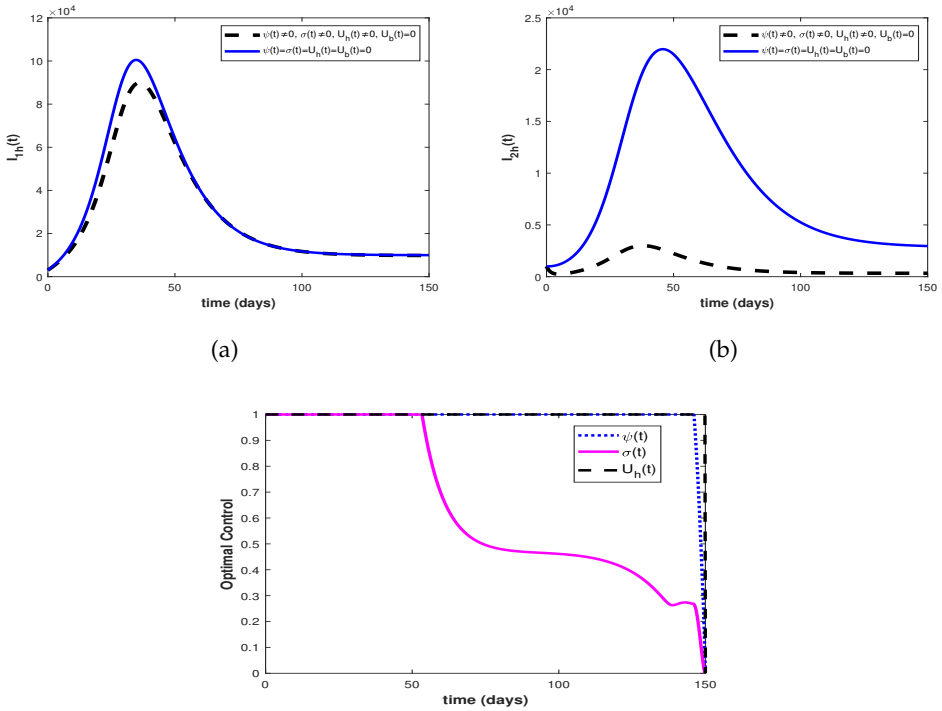

FIGURE 9. Behavior of avian influenza system (4.1) in the presence of optimal combination of interventions $\psi(t), \sigma(t)$ and $U_h(t)$.

encouraged to successfully fight against the spread of influenza in the population. In addition, a drastic reduction is noticed in the population size of the infectious birds when the controls are in place compared to the case when their is no consideration for control interventions. This emphasizes the importance of including culling of infected birds in the fight against the spread of the disease in avian population. The control profile given in Figure 10(d) shows that all the interventions should be maximally maintained at 100% within the first 2 days, 10 days, and 145 days of the implementation period before retracing to zero in the final time. In a related approach, Figure 11 shows the impact of the optimal implementation of control interventions $\psi(t)$, $U_h(t)$ and $U_b(t)$ on the infectious populations of the influenza model (4.1). One sees that the population sizes of the infectious human and birds reduced significantly when intervention strategies are implemented. Figure 11(d) is the pictorial representation of the control profile for the interventions and it is shown that optimal implementation of interventions $\psi(t)$ and $U_h(t)$ should be encouraged at maximum 100% throughout the entire period of implementation, while control $U_b(t)$ should be kept optimally within the first 10 days of implementation to guarantee optimal result.

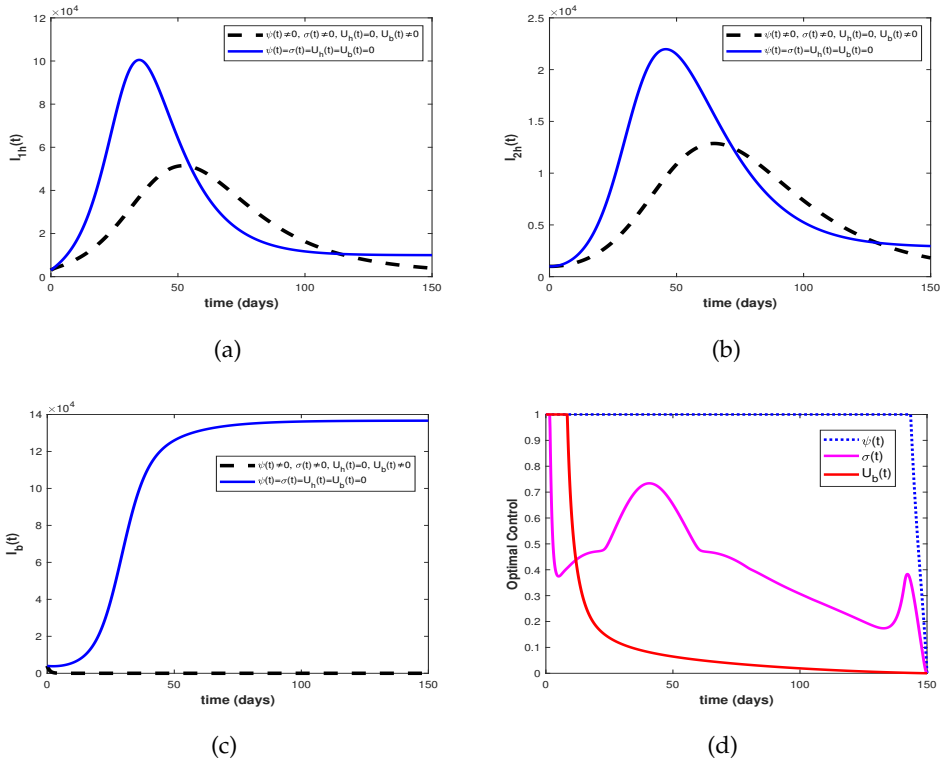

FIGURE 10. Effect of combination of control interventions $\psi(t), \sigma(t)$ and $U_b(t)$ on the avian influenza system (4.1).

Moreover, Figure 12 shows the most significant reduction in the numbers of populations of non-isolated and isolated infectious humans and infectious birds accordingly, when control interventions $\sigma(t)$, $U_h(t)$ and $U_b(t)$ are implemented. This affirms the need to combine vaccination, anti-viral treatment and culling in order to successfully hamper the spread of avian influenza in the population. The control profile depicting the optimal implementation of the interventions $\sigma(t)$, $U_h(t)$ and $U_b(t)$ shows that optimal solution is achievable if the interventions σ and U_b could be optimally maintained at maximum 100% within the first 10 days and 120 days of implementation before gradually reducing to zero in the final time. Whereas, control $U_h(t)$ must be kept at the upper bound throughout the implementation period.

5. CONCLUSION

In this study, a new deterministic mathematical model governed by a system of nonlinear ordinary differential equations for the transmission dynamics of avian influenza virus has been formulated and analysed. The developed model requires the interaction between human and avian (bird) populations, therefore, the model describes how avian influenza spread affects the total human and bird populations using the concept of a simple Susceptible-Infectious-Recovered model. The model stratified the susceptible class into the population of uninformed and informed individuals and the infectious population is sub-categorized into isolated and non-isolated individuals.

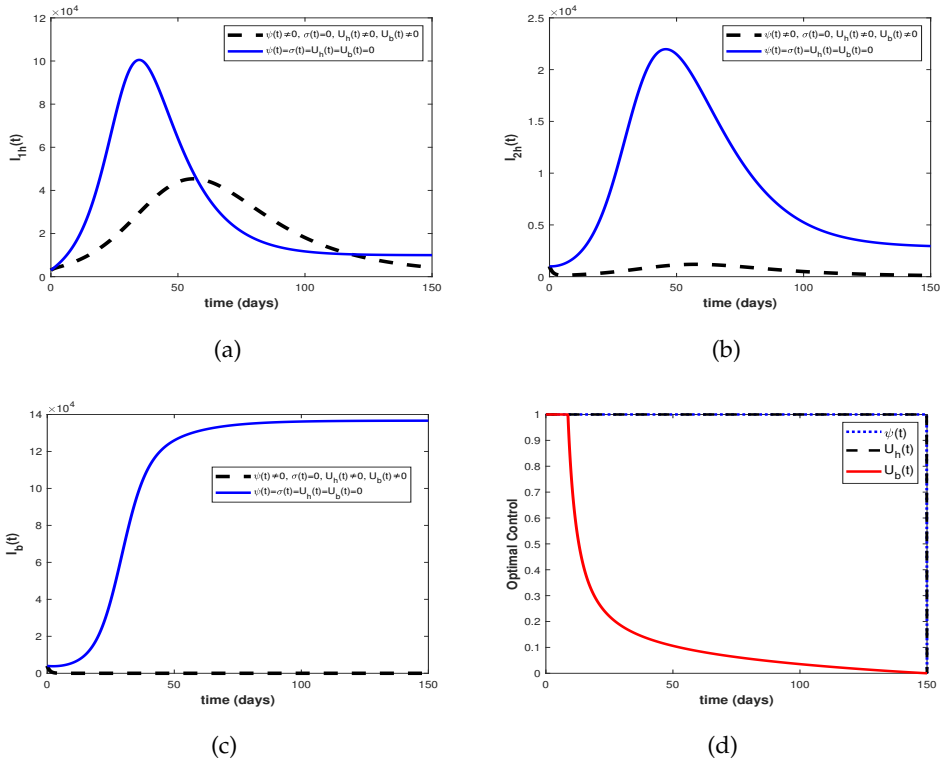

FIGURE 11. Behavior of the avian influenza system (4.1) in the presence of optimal combination of interventions $\psi(t), U_h(t)$ and $U_b(t)$.

Thus, the total human population on the one hand is stratified into six mutually exclusive classes, including uninformed susceptible class, informed susceptible class, vaccinated class, non-isolated infectious population, isolated infectious compartment, and recovered class. While the total birds population on the other hand is subdivided into susceptible and infectious compartments. The model was qualitatively analysed based on the application of dynamical systems methodologies and optimal control theory.

The autonomous influenza model was shown to have a globally asymptotically stable disease-free equilibrium point when the effective reproduction number is less than unity. Moreover, the avian influenza model was shown to have a unique endemic equilibrium point, which is globally asymptotically stable when the effective reproduction number is more than unity.

The analysis of the control dynamical system with four time-dependent control interventions, namely precautionary education, vaccination, treatment control with anti-viral drugs and culling of infected birds in the flock, was explored to examine the behavior of trajectories of infectious humans and birds in comparison with the case without controls. The combinations of any three control strategies were considered, and it was observed that the presence of each control combination has the ability to stem down the magnitudes of non-isolated infectious, isolated infectious individuals as well as the infectious birds in the population at minimum cost of control implementation. In

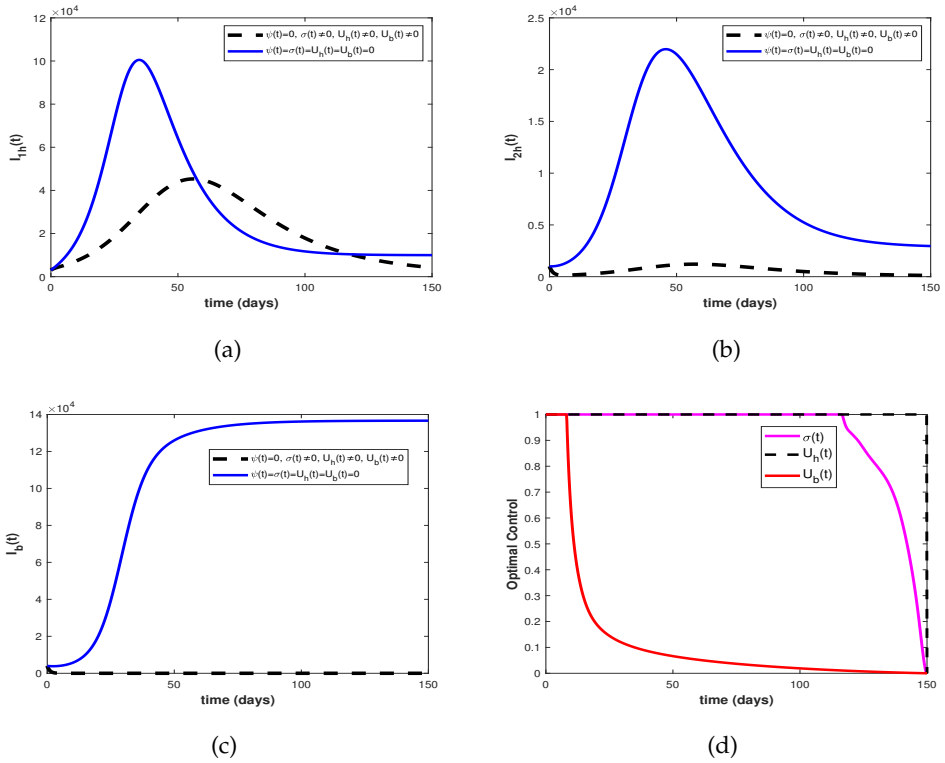

FIGURE 12. Behavior of the avian influenza model (4.1) in the presence of optimal combination of interventions $\sigma(t), U_h(t)$ and $U_b(t)$.

particular, it was discovered that the potential spread of avian influenza could be significantly curbed in the population if intervention efforts such as vaccination, isolation with treatment and culling of sick birds could be combined and optimally implemented.

Conflicts of Interest: The authors declare that there are no conflicts of interest regarding the publication of this paper.

REFERENCES

[1] R.G. Webster, W.J. Bean, O.T. Gorman, T.M. Chambers, Y. Kawaoka, Evolution and Ecology of Influenza A Viruses, Microbiol. Rev. 56 (1992), 152–179. https://doi.org/10.1128/mr.56.1.152-179.1992.

[2] C. Modnak, Mathematical Modelling of an Avian Influenza: Optimal Control Study for Intervention Strategies, Appl. Math. Inf. Sci. 11 (2017), 1049–1057. https://doi.org/10.18576/amis/110411.

[3] World Health Organization, Avian Influenza, 2024. https://www.who.int/westernpacific/wpro-emergencies/surveillance/avian-influenza.

[4] CDC, Key Facts about Avian Influenza (Avian Flu) and Highly Pathogenic Avian Influenza A (H5N1) Virus, Centers for Disease Control and Prevention, 2024.

[5] WHO, Global Influenza Report, World Health Organization, 2018.

[6] N.S. Chong, J.M. Tchuenche, R.J. Smith, A Mathematical Model of Avian Influenza with Half-Saturated Incidence, Theory Biosci. 133 (2014), 23–38. https://doi.org/10.1007/s12064-013-0183-6.

[7] J.K. Taubenberger, D.M. Morens, 1918 Influenza: The Mother of All Pandemics, Emerg. Infect. Dis. 12 (2006), 15–22. https://doi.org/10.3201/eid1201.050979.

[8] A.B. Gumel, Global Dynamics of a Two-Strain Avian Influenza Model, Int. J. Comput. Math. 86 (2009), 85–108. https://doi.org/10.1080/00207160701769625.

[9] M.A. Khan, M. Farhan, S. Islam, et al. Modeling the Transmission Dynamics of Avian Influenza with Saturation and Psychological Effect, Discrete Contin. Dyn. Syst. S 12 (2019), 455–474. https://doi.org/10.3934/dcdss.2019030.

[10] M.A. Khan, S. Ullah, Y. Khan, M. Farhan, Modeling and Scientific Computing for the Transmission Dynamics of Avian Influenza with Half-Saturated Incidence, Int. J. Model. Simul. Sci. Comput. 11 (2020), 2050035. https://doi.org/10.1142/S179396232050035X.

[11] X. Jiang, Y. Yu, F. Meng, et al. Modelling the Dynamics of Avian Influenza With Nonlinear Recovery Rate and Psychological Effect, J. Appl. Anal. Comput. 10 (2020), 1170–1192. https://doi.org/10.11948/20190253.

[12] M.H. Alharbi, C.M. Kribs, A Mathematical Modeling Study: Assessing Impact of Mismatch Between Influenza Vaccine Strains and Circulating Strains in Hajj, Bull. Math. Biol. 83 (2021), 7. https://doi.org/10.1007/s11538-020-00836-6.

[13] I.A. Baba, H. Ahmad, M.D. Alsulami, et al. A Mathematical Model to Study Resistance and Non-Resistance Strains of Influenza, Results Phys. 26 (2021), 104390. https://doi.org/10.1016/j.rinp.2021.104390.

[14] M. Barik, C. Swarup, T. Singh, et al. Dynamical Analysis, Optimal Control and Spatial Pattern in an Influenza Model with Adaptive Immunity in Two Stratified Population, AIMS Math. 7 (2022), 4898–4935. https://doi.org/10.3934/math.2022273.

[15] Z. Du, S.J. Fox, T. Ingle, et al. Projecting the Combined Health Care Burden of Seasonal Influenza and COVID-19 in the 2020–2021 Season, MDM Policy Pract. 7 (2022), 23814683221084631. https://doi.org/10.1177/23814683221084631.

[16] T. Zheng, L. Nie, H. Zhu, et al. Role of Seasonality and Spatial Heterogeneous in the Transmission Dynamics of Avian Influenza, Nonlinear Anal.: Real World Appl. 67 (2022), 103567. https://doi.org/10.1016/j.nonrwa.2022.103567.

[17] R. Sachak-Patwa, E.I. Lafferty, C.J. Schmit, et al. A Target-Cell Limited Model Can Reproduce Influenza Infection Dynamics in Hosts with Differing Immune Responses, J. Theor. Biol. 567 (2023), 111491. https://doi.org/10.1016/j.jtbi.2023.111491.

[18] H. Gourram, M. Baroudi, A. Labzai, M. Belam, Mathematical Modeling and Optimal Control Strategy for the Influenza (H5N1), Commun. Math. Biol. Neurosci. 2023 (2023), 113. https://doi.org/10.28919/cmbn/8199.

[19] A. Malek, A. Hoque, Mathematical Modeling of the Infectious Spread and Outbreak Dynamics of Avian Influenza with Seasonality Transmission for Chicken Farms, Comparative Immunology, Microbiol. Infect. Dis. 104 (2024), 102108. https://doi.org/10.1016/j.cimid.2023.102108.

[20] F. Pinotti, L. Kohnle, J. Lourenço, et al. Modelling the Transmission Dynamics of H9N2 Avian Influenza Viruses in a Live Bird Market, Nat. Commun. 15 (2024), 3494. https://doi.org/10.1038/s41467-024-47703-9.

[21] C. Andreu-Vilarroig, R.J. Villanueva, G. González-Parra, Mathematical Modeling for Estimating Influenza Vaccine Efficacy: A Case Study of the Valencian Community, Spain, Infect. Dis. Model. 9 (2024), 744–762. https://doi.org/10.1016/j.idm.2024.04.006.

[22] Y. Chen, J. Zhang, Dynamic Analysis and Optimal Control of Influenza Model with Discrete Age Structure, Math. Methods Appl. Sci. 47 (2024), 4260–4282. https://doi.org/10.1002/mma.9813.

[23] S.F. Abimbade, S. Olaniyi, O.A. Ajala, Recurrent Malaria Dynamics: Insight from Mathematical Modelling, Eur. Phys. J. Plus 137 (2022), 292. https://doi.org/10.1140/epjp/s13360-022-02510-3.

[24] P. Van Den Driessche, J. Watmough, Reproduction Numbers and Sub-Threshold Endemic Equilibria for Compartmental Models of Disease Transmission, Math. Biosci. 180 (2002), 29–48. https://doi.org/10.1016/S0025-5564(02)00108-6.

[25] O.D. Falowo, S. Olaniyi, A.T. Oladipo, Optimal Control Assessment of Rift Valley Fever Model with Vaccination and Environmental Sanitation in the Presence of Treatment Delay, Model. Earth Syst. Environ. 9 (2023), 457–471. https://doi.org/10.1007/s40808-022-01508-1.

[26] S. Olaniyi, S.F. Abimbade, F.M. Chuma, O.A. Adepoju, O.D. Falowo, A Fractional-Order Tuberculosis Model with Efficient and Cost-Effective Optimal Control Interventions, Decis. Anal. J. 8 (2023), 100324. https://doi.org/10.1016/j.dajour.2023.100324.

[27] A.D. Polyanin, A.V. Manzhirov, Handbook of Mathematics for Engineers and Scientists, Chapman & Hall/CRC, (2007).

[28] O.S. Obabiyi, S. Olaniyi, Asymptotic Stability of Malaria Dynamics With Vigilant Human Compartment, Int. J. Appl. Math. 29 (2016), 127-144. https://doi.org/10.12732/ijam.v29i1.10.

[29] C. Castillo-Chavez, P. Blower, P. van den Driessche, W. Kirschner, A. Yakubu, Mathematical Approaches for Emerging and Reemerging Infectious Diseases: An Introduction, Springer, 2002.

[30] S. Olaniyi, G.G. Kareem, S.F. Abimbade, F.M. Chuma, S.O. Sangoniyi, Mathematical Modelling and Analysis of Autonomous HIV/AIDS Dynamics with Vertical Transmission and Nonlinear Treatment, Iran. J. Sci. 48 (2024), 181–192. https://doi.org/10.1007/s40995-023-01565-w.

[31] S.F. Abimbade, F.M. Chuma, S.O. Sangoniyi, et al. Global Dynamics of a Social Hierarchy-Stratified Malaria Model: Insight from Fractional Calculus, Mathematics 12 (2024), 1593. https://doi.org/10.3390/math12101593.

[32] M.A. Rois, Fatmawati, C. Alfiniyah, S. Martini, D. Aldila, F. Nyabadza, Modeling and Optimal Control of COVID-19 with Comorbidity and Three-Dose Vaccination in Indonesia, J. Biosaf. Biosecurity 6 (2024), 181–195. https://doi.org/10.1016/j.jobb.2024.06.004.

[33] J.P. La Salle, The Stability of Dynamical Systems, SIAM, 1976. https://doi.org/10.1137/1.9781611970432.

[34] L.S. Pontryagin, V.G. Boltyanskii, Mathematical Theory of Optimal Processes, Wiley, 1962.

[35] J.K.K. Asamoah, E. Yankson, E. Okyere, et al. Optimal Control and Cost-Effectiveness Analysis for Dengue Fever Model with Asymptomatic and Partial Immune Individuals, Results Phys. 31 (2021), 104919. https://doi.org/10.1016/j.rinp.2021.104919.

[36] O.F. Lawal, T.T. Yusuf, A. Abidemi, On Mathematical Modelling of Optimal Control of Typhoid Fever with Efficiency Analysis, J. Nigerian Soc. Phys. Sci. 6 (2024), 2057. https://doi.org/10.46481/jnsps.2024.2057.

[37] O. Boukary, Z. Malicki, G. Elisée, Mathematical Modeling and Optimal Control of an HIV/AIDS Transmission Model, Int. J. Anal. Appl. 22 (2024), 234. https://doi.org/10.28924/2291-8639-22-2024-234.

[38] F.B. Agusto, Optimal Isolation Control Strategies and Cost-Effectiveness Analysis of a Two-Strain Avian Influenza Model, Biosystems 113 (2013), 155–164. https://doi.org/10.1016/j.biosystems.2013.06.004.

[39] S. Edward, N. Shaban, Deterministic Compartmental Model for Optimal Control Strategies of Giardiasis Infection with Saturating Incidence and Environmental Dynamics, Healthc. Anal. 7 (2025), 100383. https://doi.org/10.1016/j.health.2025.100383.

[40] S. Olaniyi, J.O. Olayiwola, O.S. Obabiyi, R.S. Lebelo, S.F. Abimbade, Mathematical Analysis of Non-Autonomous HIV/AIDS Transmission Dynamics with Efficient and Cost-Effective Intervention Strategies, Contemp. Math. 6 (2025), 1380–1400. https://doi.org/10.37256/cm.6220256138.

[41] H.A. Engida, D. Fisseha, Malaria and Leptospirosis Co-Infection: A Mathematical Model Analysis with Optimal Control and Cost-Effectiveness Analysis, Sci. Afr. 27 (2025), e02517. https://doi.org/10.1016/j.sciaf.2024.e02517.

[42] N.K. Goswami, S. Olaniyi, S.F. Abimbade, F.M. Chuma, A Mathematical Model for Investigating the Effect of Media Awareness Programs on the Spread of COVID-19 with Optimal Control, Healthc. Anal. 5 (2024), 100300. https://doi.org/10.1016/j.health.2024.100300.

[43] S. Barman, S. Jana, S. Majee, D.K. Das, T.K. Kar, Complex Dynamics of a Fractional-Order Epidemic Model with Saturated Media Effect, Nonlinear Dyn. 112 (2024), 18611–18637. https://doi.org/10.1007/s11071-024-09932-x.

[44] S. Lenhart, J.T. Workman, Optimal Control Applied to Biological Models, Chapman & Hall, London, (2007).

[45] S. Olaniyi, S.F. Abimbade, O.A. Ajala, F.M. Chuma, Efficiency and Economic Analysis of Intervention Strategies for Recurrent Malaria Transmission, Qual. Quant. 58 (2024), 627–645. https://doi.org/10.1007/s11135-023-01664-1.